

# Sodium tungstate immobilized on plasma-treated PVDF membranes: New efficient heterogeneous catalyst for oxidation of secondary amines to nitrones

M.G. Buonomenna<sup>a,\*</sup>, L.C. Lopez<sup>b</sup>, G. Barbieri<sup>a</sup>, P. Favia<sup>b,c</sup>, R. d'Agostino<sup>b,c</sup>, E. Drioli<sup>a</sup>

<sup>a</sup> Institute on Membrane Technology, National Research Council of Italy, ITM-CNR, c/o University of Calabria,  
via P. Bucci cubo 17/C, 87030 Rende (CS), Italy

<sup>b</sup> Department of Chemistry, University of Bari, via Orabona 4, 70126 Bari, Italy

<sup>c</sup> Institute of Inorganic Methodologies and Plasmas IMIP-CNR, via Orabona 4, 70126 Bari, Italy

Received 11 January 2006; received in revised form 18 March 2007; accepted 21 March 2007

Available online 27 March 2007

## Abstract

New heterogeneous oxidation catalysts have been obtained by immobilizing sodium tungstate ( $\text{Na}_2\text{WO}_4$ ) on plasma-treated poly(vinylidene difluoride) (PVDF) membranes. This new generation of catalytically active membranes has been developed by coupling the advantages of low temperature plasma modification processes with surface chemical immobilization reactions of catalysts. Polymeric membranes with different thicknesses, morphologies and pore dimensions were prepared by a non-solvent induced phase inversion technique. Then the surface of the membranes have been surface modified with  $\text{NH}_3$  radiofrequency glow discharges in order to graft active amino groups for immobilizing sodium tungstate in a stable way. The new catalytic membranes were successfully used for the oxidation of secondary amines to nitrones in a flat membrane reactor. A conversion to nitronone of 100% in less than 3 h (comparable to the homogeneous system) was achieved with the membrane having smallest pore diameter and finger like morphology.

© 2007 Elsevier B.V. All rights reserved.

**Keywords:** Catalytic polymeric membranes; Membrane reactors; Poly(vinylidene difluoride); Plasma treatment

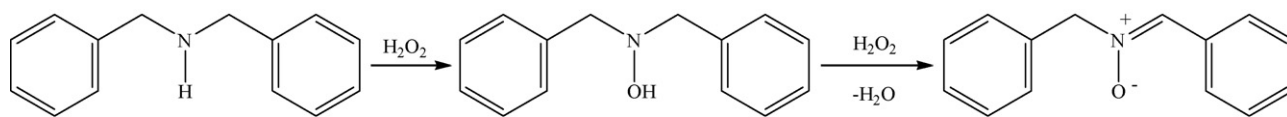
## 1. Introduction

The current trend towards a sustainable chemistry has given life to an increasing number of new strategies for catalyst immobilization, enabling an easy recovery, re-use and disposal at low cost of the catalyst. To this category belong catalytic polymeric membranes in which no catalyst recovery is required, reaction and separation of the products are coupled, catalysts may have longer life and the intact structure of the catalyst should be preserved inside the polymeric membranes, minimizing any change in activity and selectivity in comparison with the homogeneous system [1–4]. In particular, in biomimetic chemistry, the application of new materials has been extensively studied in order to prepare catalysts that are more stable and selective under the employed reaction conditions [5]. The first room

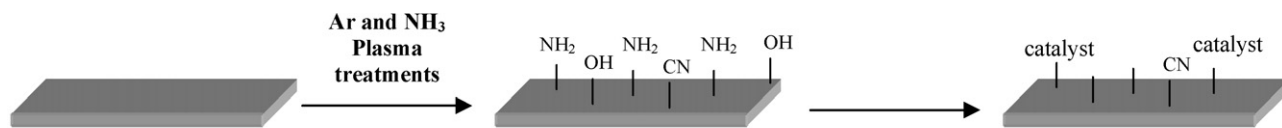
temperature catalytic membrane was realised by embedding the Fe–Pc–Y catalyst in a hydrophobic PDMS (polydimethylsiloxane) membrane: the supramolecular catalyst strongly resembled the architecture of natural cytochrome P-450. In fact, in living eucaryotic cells, cytochrome P-450 is embedded in phospholipid membranes, which act as a reservoir for reactants. In catalytic polymeric membranes, the polymeric membrane takes over the role of this phospholipid double layer, like the catalytic complex of the enzyme [6–8]. We have recently reported that titanatrane complex was successfully entrapped in polymeric membranes based on polyvinylidene difluoride (PVDF) and used in the oxidation of secondary amines to nitrones [9] (Scheme 1).

The oxidation of amines to nitrones is a very appealing reaction because of both the relevance of the metabolic fate of these compounds *in vivo* and of the synthetic interest of the reaction products. Important enzymes are involved in the metabolic oxidation of amines. For example, flavin mono-oxygenase and related compounds such as 5-ethyl-4a-hydro-peroxyflavin oxidize secondary amines to nitrones [10]. The mimicry of the

\* Corresponding author. Tel.: +39 0984492014; fax: +39 0984402103.  
E-mail address: [mg.buonomenna@itm.cnr.it](mailto:mg.buonomenna@itm.cnr.it) (M.G. Buonomenna).



Scheme 1.



PVDF membranes

Scheme 2.

activity of these enzymes using metal complexes is of great interest, potentially providing mimetic methods for catalytic oxidation of the amines [11].

In this work, a new generation of catalytically active membranes for secondary amines oxidation has been developed by coupling the advantages of low temperature plasma modification processes with surface chemical immobilization of W-based catalysts. Plasma treatments in  $\text{NH}_3$  fed radio frequency (rf) (13.56 MHz) glow discharges have been used to generate functionalized PVDF membranes suitable for the immobilization of  $\text{Na}_2\text{WO}_4$ . As shown in Scheme 2, the catalyst is immobilized on the membrane surface.

The new catalytically active membranes, obtained with this innovative catalyst immobilization technique [12], were applied in the oxidation of secondary amines to nitrones in a flat membrane reactor. The different experiments were focused on the study of the effect of the membrane thickness and pore dimensions on reagent conversion and selectivity. The polymeric catalytic membranes studied in this work were characterized by different morphologies (finger-like and nodular-sponge-like), porosities and pore dimensions ranging from 0.06 to 0.25  $\mu\text{m}$ . We observed that the activity of the new catalytic membranes depended on the pore dimensions.

## 2. Experimental

### 2.1. General remarks

Commercially available reagents and solvents were used as received without further purification. PVDF polymer was supplied from Solef, under the trade name of Solef 6010.

### 2.2. Catalytic polymeric membranes

#### 2.2.1. Preparation

Flat sheet PVDF were prepared by a non-solvent induced phase inversion process. The membranes were prepared using dimethyl acetamide (DMA) as solvent and distilled water as non-solvent. The solution was cast on a glass plate by setting the knife gap at 250  $\mu\text{m}$  and the cast film was immediately immersed in a coagulation bath containing distilled water at 15  $^\circ\text{C}$ .

The different membrane preparation conditions (polymeric solution concentrations, temperature and coagulation

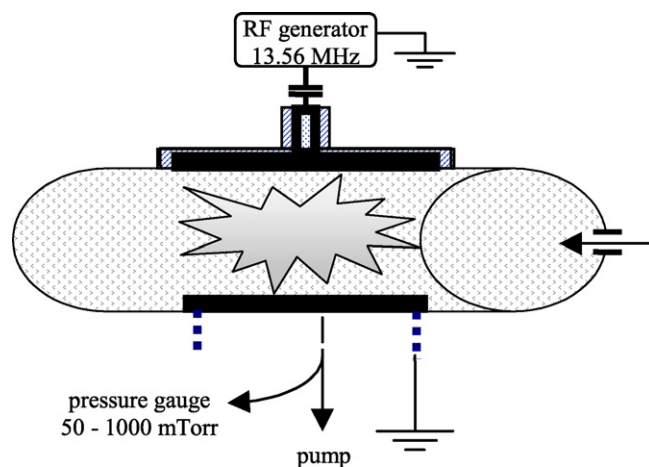
bath composition) were described in more details elsewhere [13].

Plasma treatments have been performed in a quasiparallel plate glass tubular pyrex reactor in the parallel plate configuration equipped with a set of two electrodes. Discharges were set between two horizontal “parallel plate” steel electrodes; the upper external electrode (cathode) was conformal to the reactor and connected to a rf generator (ENI-ACG-10 operating at 13.56 MHz) through an impedance matching network and the lower internal electrode was used as membranes holder connected to the ground (Scheme 3).

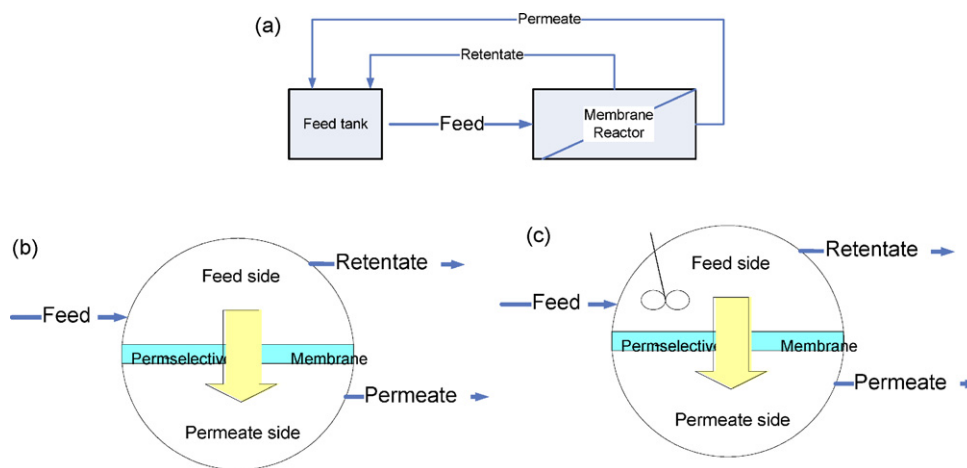
The gases were let to the chamber through a controlled system of MKS<sup>®</sup> flowmeters calibrated according to the gas used. A rotary pump was used to evacuate the chamber and the pressure was controlled with a MKS Baratron manometer.

Membranes were first plasma-treated in glow discharge fed with Ar (20 sccm, 800 mTorr of pressure, 30 W, 1 min), in order to induce a cross-linking of activated species by inert gases (CASING). Ar-treated membranes were subsequently plasma-treated in  $\text{NH}_3$  rf glow discharge (20 sccm, 300 mTorr of pressure, 20 W, 5 min) to obtain N-containing groups grafted on a surface more stable to ageing as will be shown below.

The catalyst  $\text{Na}_2\text{WO}_4 \cdot 2\text{H}_2\text{O}$  has been dissolved in distilled water to a 0.1 M solution (pH approximately 10.0). This solution has been acidified with a 0.5 M HCl solution up to pH 5.



Scheme 3.



Scheme 4.

### 2.2.2. Characterization

The chemical composition of native and modified PVDF membranes has been determined by XPS using a PHI ESCA 5300 instrument equipped with a non-monochromatic Mg  $K\alpha$  radiation (1253.6 eV). The measurements have been performed at a take-off angle fixed at  $45^\circ$  (sampling depth  $\sim 7$  nm). During analysis the pressure has been around  $10^{-8}$  Torr. Low resolutions (pass energy 89.45 eV; 0–1000 eV) and higher resolution (pass energy 34.75 eV; C 1s, O 1s, N 1s, F 1s, W 4f regions) spectra have been acquired for qualitative and quantitative surface analysis.

The membrane thicknesses were determined by a digital micrometer (Carl Mahr D 7300.) and by SEM observation of the freeze-fractured cross sections. Membrane pore dimensions was characterized by a capillary flow porometer CFP 1500 AEXL (Porous materials Inc., USA). The morphology of the membranes dried at  $60^\circ\text{C}$  overnight was examined using SEM, Cambridge, Stereoscan 360, at 20 kV. For cross-section analysis the membrane samples were freeze-fractured in liq-

uid nitrogen. All samples were sputter-coated with gold before analysis.

### 2.3. Testing procedure of catalytic polymeric membranes

The performance of the catalytic membranes was investigated using a flat membrane reactor operating in a recirculation mode (Scheme 4a) in two different ways: without (Scheme 4b) or with (Scheme 4c) stirring in the membrane feed side. The feed tank was loaded with a dibenzylamine solution in methanol (0.19 M, 25 mL) and recirculated for 10 min; then at  $0^\circ\text{C}$  hydrogen peroxide (1.7 g, 30% (v/v)) was added. The tests were carried out at  $25^\circ\text{C}$  operating at  $\Delta P = 0\text{--}1$  bar. Performance of the catalytic membranes was tested both in “flow through” and contact modes.

Reaction species were continuously monitored by analyzing the feed tank solution during the course of reaction with UV (dibenzylamine at 240 nm and the product at 295 nm [11]). Because the molar absorptivity of the nitrones is so large,

Table 1  
Characteristics of PVDF catalytic membranes

| Membrane | Thickness ( $\mu\text{m}$ ) | Pore dimension ( $\mu\text{m}$ ) |                |              | Porosity (%) |
|----------|-----------------------------|----------------------------------|----------------|--------------|--------------|
|          |                             | Smallest pore                    | Mean flow pore | Largest pore |              |
| M1       | 46.7                        | 0.055                            | 0.06           | 0.2          | 6.82         |
| M2       | 52.0                        | –                                | 0.09           | 1.2          | 18.36        |
| M3       | 20.2                        | –                                | 0.13           | 0.49         | 26.2         |
| M4       | 24.8                        | –                                | 0.25           | 0.59         | 35.0         |

Table 2  
Surface composition from XPS data of chemically modified membranes

| Substrate                   | C%   | O%   | W 4f% | F%   | N%  | O/C  | N/C  | W/C  | F/C  |
|-----------------------------|------|------|-------|------|-----|------|------|------|------|
| PVDF native                 | 52.1 | 1.7  | –     | 46.3 | –   | 0.03 | –    | –    | 0.89 |
| PVDF/Ar                     | 66.2 | 5.8  | –     | 24.5 | 3.5 | 0.09 | 0.05 | –    | 0.37 |
| PVDF/Ar/NH <sub>3</sub>     | 64.5 | 2.6  | –     | 24.1 | 8.7 | 0.04 | 0.13 | –    | 0.37 |
| PVDF/Ar/NH <sub>3</sub> /W1 | 61.2 | 13.2 | 2.8   | 17.7 | 5.1 | 0.21 | 0.08 | 0.04 | 0.29 |

$\sim 1.2 \times 10^4 \text{ L mol}^{-1} \text{ cm}^{-1}$ , a cell of 0.02 cm was used to keep the absorbance changed within a permissible range.

### 3. Results and discussion

#### 3.1. Catalytic functionalized membranes

Four PVDF catalytic membranes characterized by different thicknesses, pore dimensions and morphologies were tested. The mean flow pore diameter ranged from 0.06 to 0.25  $\mu\text{m}$  (Table 1).

The pore size distribution (Fig. 1) was characterized by SCION IMAGE analysis of SEM images of membrane surfaces.

In Fig. 2 the morphology of the different membranes is shown. M1 and M2 are characterized by a finger-like morphology with elongated macrovoids across membrane sections. A thick skin layer and a porous sublayer are visible for both polymeric membranes. The membrane surfaces are smooth and characterized by an homogeneous pore distribution (Fig. 2(a and b)). M3 and M4 have very different morphologies as can be seen in Fig. 2(c and d); the cross sections are porous nearly symmetric nodular characterized by a very thin skin layer on an open

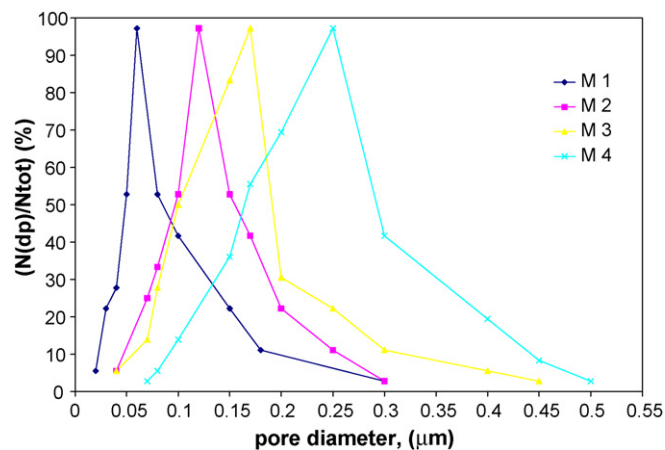


Fig. 1. Pore diameter distribution for the four PVDF membranes.

sponge sublayer. Uniform pore distribution on the membrane surfaces is visible at a magnification of 1000.

To explain results from the various surface modification experiments, the following definitions have been adopted: PVDF/ $\text{NH}_3$  (PVDF membrane-treated in an  $\text{NH}_3$  rf glow

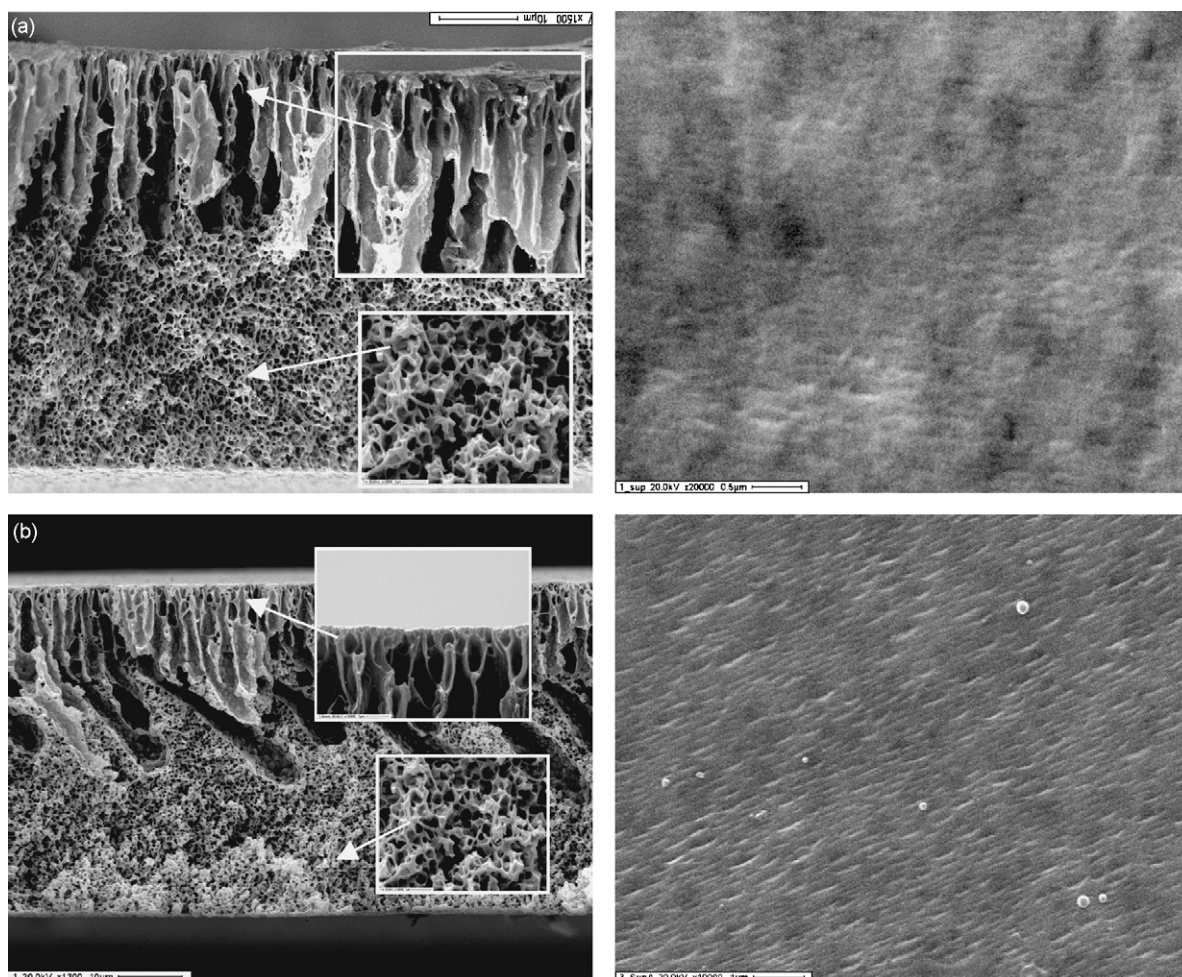


Fig. 2. SEM images of cross sections (left) and top surface (right) of (a) M1, (b) M2. SEM images of cross sections (left) and top surface (right) of (c) M3 and (d) M4.

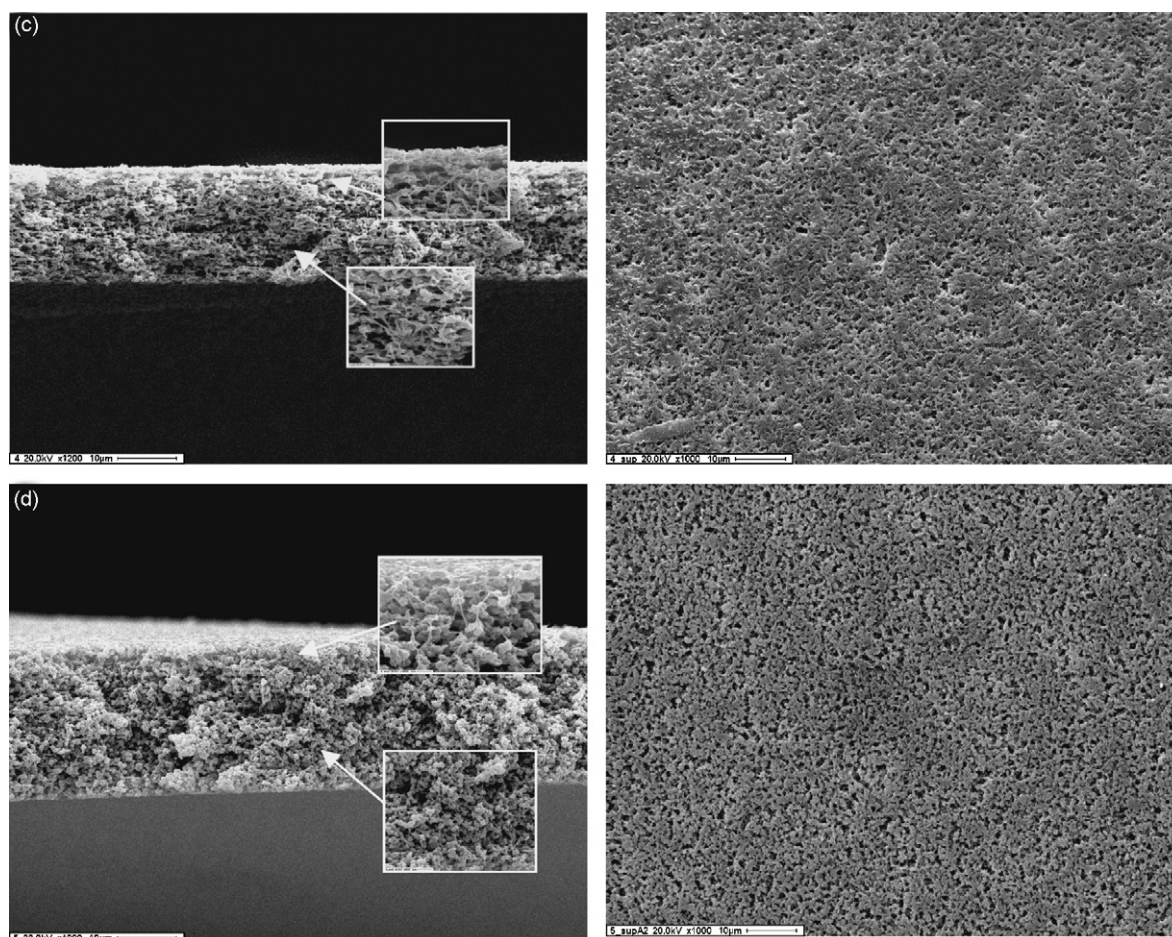
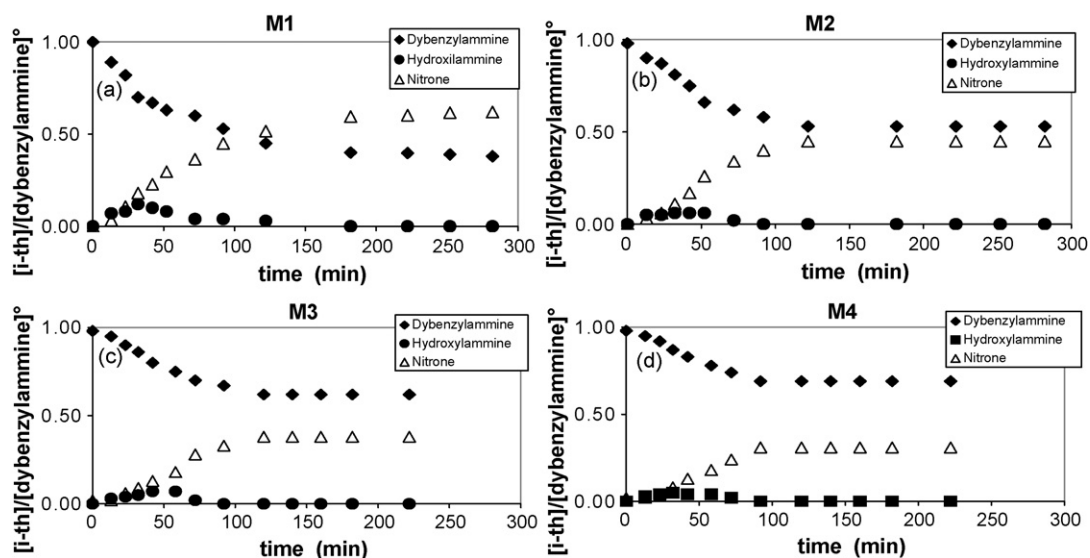


Fig. 2. (Continued).

discharge); PVDF/Ar/NH<sub>3</sub> (PVDF membrane pre-treated in an Ar fed rf glow discharge then treated in an NH<sub>3</sub> glow discharge); PVDF/Ar/NH<sub>3</sub>/W1 (PVDF/Ar/NH<sub>3</sub> with Na<sub>2</sub>WO<sub>4</sub> catalyst immobilized).

Evidence of the immobilization of the W-containing catalysts on PVDF/Ar/NH<sub>3</sub>/W surface has been obtained through X-ray photoelectron spectroscopy (XPS); the characterization has been performed after each step of modification. XPS results revealed

Fig. 3. Conversion of the reagents monitored during the reaction course using (a) M1, (b) M2, (c) M3 and (d) M4.  $T = 25^\circ\text{C}$ ;  $\Delta P = 1$  bar.

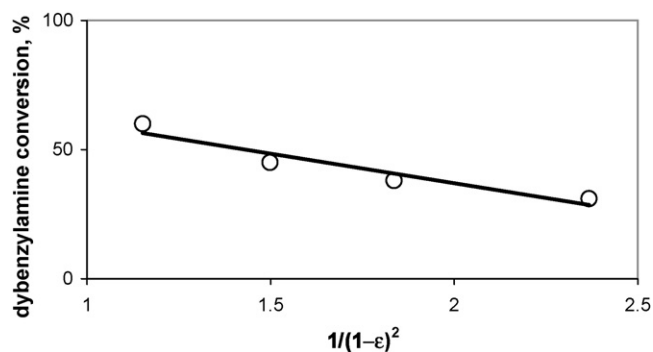


Fig. 4. Dibenzylamine conversion against  $1/(1-\varepsilon)^2$ .

the presence of tungsten after the immobilization procedure as shown in Table 2. Ar plasma pre-treatments caused a severe defluorination of the PVDF surface evidenced from the decrease in the F 1s/C 1s elemental ratio from 0.90 to 0.37 (Table 2).

After W1 immobilization a consistent enhancement of the oxygen content has been recorded in elemental composition; the O/C ratio increases from 0.03 to 0.21. The increase in the oxygen content reflects the number of oxygen atoms present in the W1.

### 3.2. Membrane reactivity

Measured conversion profiles of the reactants are shown in Fig. 3(a–d). Using catalytic membrane M1, the formation of nitron and the corresponding decrease in the substrate, i.e. dibenzylamine, was observed; after 180 min the conversion reached a plateau value of 60%. The conversion to nitron decreased with M2, M3 and M4. The plateau is reached at 120 min due to the lower conversions. In the oxidation of secondary amines catalyzed by free tungstate after 3 h of reaction, the nitron yield was 85% [14].

From these conversion results, we can establish the following reactivity trend for the four catalytic membranes: M1 > M2 > M3 > M4. This trend reflects the relative membrane pore dimensions and porosity: the membrane pore dimension (as shown in Table 1) increases from 0.01 for M1 to 0.25  $\mu\text{m}$  for M4. Fig. 4 shows the plot of conversion values obtained with the four membranes against  $1/(1-\varepsilon)^2$ , where  $\varepsilon$  is the membrane porosity. It is noteworthy that the relationship is linear and therefore reflects the flux equation of Kozeny–Carman. As is well known, Kozeny–Carman Eq. (1) describes the system of closed packed

spheres that can be found in phase inversion membranes with a nodular top layer structure

$$J = \frac{\varepsilon^3}{K\eta S^2(1-\varepsilon)^2} \frac{\Delta P}{\Delta X} \quad (1)$$

Eq. (1) indicates that the solvent flux ( $J$ ) is proportional to the driving force, i.e. the pressure difference ( $\Delta P$ ) across a membrane of thickness  $\Delta X$  and inversely proportional to the viscosity  $\eta$ . The quantity  $S$  is the internal surface area, and  $K$  the Kozeny–Carman constant, which depends on the shape of the pores and the tortuosity.

The relationship found between the observed conversions and  $1/(1-\varepsilon)^2$  suggests that with decreasing membrane surface porosity, more active catalyst sites become available on the membrane surface: this fact is consequent upon the surface immobilization of the catalyst, which did not occur inside the membrane pores. Moreover, the linear trend according to the Kozeny–Carman equation indicates that a low  $\Delta P$  must be used in order to facilitate the contact between reagent and membrane surface, i.e. to decrease the flux across the membrane.

Therefore, next experiments were carried out with the flux across membrane decreased, i.e. at  $\Delta P=0$  and by using membrane M1, which has the smallest pore dimension surface porosity. In this case, two types of experiments were carried out: with and without stirring on the feed side. For both cases, plot of conversion versus time is shown in Fig. 5. In both cases an increase in conversion is observed compared to the values obtained at  $\Delta P=1$  bar (60%): 70% without stirring and 100% with stirring.

It is noteworthy that with stirring the conversion increases up to 100%. At  $\Delta P=0$  reagent diffusion and product backdiffusion are the “rate determining step” and therefore, the contact of new molecules of substrate with the catalyst immobilized on membrane surface is favoured by stirring solution on the feed side.

## 4. Conclusions

In this work we showed that the first heterogeneization of  $\text{Na}_2\text{WO}_4$  catalysts on the surface of PVDF based polymeric membranes has been successfully achieved. First, PVDF membranes have been plasma-treated with  $\text{NH}_3$  fed discharges producing surfaces rich in N-containing groups, suitable basic anchor functionalities for the immobilization of W-containing catalyst in acid solutions.

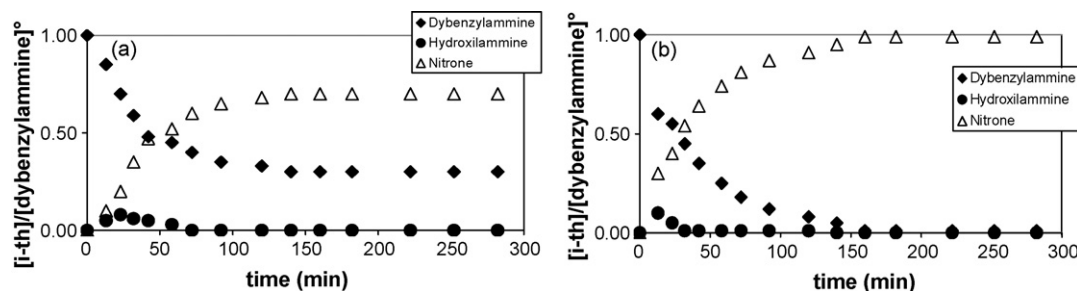


Fig. 5. Conversion of the reagents monitored during the reaction course using M1.  $T=25^\circ\text{C}$ ,  $\Delta P=0$  bar (a) without and (b) with stirring.

The reactivity screening in the model reaction of oxidation of secondary amines to nitrones of catalytic functionalized membranes characterized by different thicknesses and pore dimensions allowed us to select the membrane M1 with the lower surface porosity and pore dimension as the best catalytic membrane in terms of conversion and selectivity. The effect of two important factors affecting the process fluid dynamic has been evaluated: the transmembrane pressure and stirring in the feed membrane side. The obtained results showed that conversion increased with a transmembrane pressure  $\Delta P=0$  and stirring reaction solution on the membrane feed side.

## References

- [1] I.F.J. Vankelecom, Chem. Rev. 102 (2002) 3779.
- [2] M.C.A.F. Gotardo, A.A. Guedes, M.A. Schiavon, N.M. José, I.V.P. Yoshida, M.D. Assis, J. Mol. Catal. A: Chem. 229 (2005) 137.
- [3] R.F. Parton, I.F.J. Vankelecom, C. Casselman, P. Bezoukhanova, J.B. Uytendhoeven, P.A. Jacobs, Nature 370 (1994) 541.
- [4] I.F.J. Vankelecom, P.A. Jacobs, Catal. Today 56 (2000) 147.
- [5] P.E.F. Neys, I.F.J. Vankelecom, R.F. Parton, W. Dehaen, G. L'abbé, P.A. Jacobs, J. Mol. Catal. 126 (1997) L9.
- [6] R.F. Parton, I.F.J. Vankelecom, D. Tas, K.B. Janssen, P.P. Knops-Gerrits, P.A. Jacobs, J. Mol. Catal. 113 (1996) 283.
- [7] I.F.J. Vankelecom, D. Tas, R.F. Parton, V. Van de Vyver, P.A. Jacobs, Angew. Chem. Int. Engl. 35 (1996) 1346.
- [8] P.P. Knops-Gerrits, I.F.J. Vankelecom, E. Beatse, P.A. Jacobs, Catal. Today 32 (1996) 63.
- [9] M.G. Buonomenna, E. Drioli, G. Licini and P. Scrimin, Microreactor Technology and Process Intensification, ACS Symposium Series 914, vol. 19, American Chemical Society, Washington, 2005, p. 309.
- [10] F.P. Ballistreri, U. Chiacchio, A. Rescina, G. Tomaselli, R.M. Toscano, Tetrahedron 48 (1992) 8677.
- [11] T.H. Zauche, J.H. Espenson, Inorg. Chem. 36 (1997) 5257.
- [12] L.C. Lopez, M.G. Buonomenna, E. Fontananova, G. Iacoviello, E. Drioli, R. d'Agostino, P. Favia, Adv. Funct. Mater. 16 (2006) 1417.
- [13] M.G. Buonomenna, P. Macchi, M. Davoli, E. Drioli, Poly(vinylidene fluoride) membranes by phase inversion: the role the casting and coagulation conditions play in their morphology, crystalline structure and properties, Eur. Polym. J. 43 (4) (2007) 1557.
- [14] S.I. Murahashi, H. Mitsui, T. Shiota, T. Tsuda, S. Watanabe, J. Org. Chem. 55 (1990) 1736.